



# The role of massive AGBs in the self-enrichment scenario of globular clusters

P. Ventura

Istituto Nazionale di Astrofisica – Osservatorio Astronomico di Roma, Via Frascati 33, I-00040 Monte Porzio Catone (RM), Italy, e-mail: ventura@oa-roma.inaf.it

**Abstract.** The observed surface chemistries of globular clusters stars trace clear abundance patterns, which may be explained on the basis of a self-enrichment scenario: an early generation of intermediate mass stars, during the asymptotic giant branch evolution, might eject into the interstellar medium matter which was nuclearly processed, thus stimulating the formation of a new generation of stars, which would show the results of such pollution. To test this scenario, we calculated a new set of AGB models with the most updated physical inputs, with  $Z=0.001$ : we thus focus on the intermediate metallicity globular clusters. We show that the ejecta of the most massive models, with initial masses  $M = 5 - 6M_{\odot}$ , show up a chemistry in fairly agreement with the abundance patterns detected spectroscopically.

**Key words.** Stars: abundances – Stars: evolution

## 1. Introduction

Deep spectroscopic analysis of Globular Clusters (GC) stars show clear abundance patterns among the light elements (Kraft 1994; Carretta 2006): a not negligible percentage of stars show a strong depletion of oxygen, which, in turn, is anticorrelated with sodium and aluminium, and is correlated with fluorine and, at a smaller extent, with magnesium. The total C+N+O content is observed to be approximately constant with a factor 2 (Ivans et al. 1999). The discovery of such chemical anomalies also in TO and SGB stars (Gratton et al. 2001), and the absence of such patterns in field stars, rules out any in situ mechanism (Denissenkov & Weiss 2001) as a unique explanation, and points in favor of a self-enrichment scenario working within GCs. In

particular, an appealing explanation might be that an early generation of intermediate mass stars ( $4-6M_{\odot}$ ) evolved rapidly (100 – 200Myr), and during their Asymptotic Giant Branch (AGB) phase polluted the interstellar medium with matter which, due to Hot Bottom Burning (HBB) at the bottom of their massive convective envelope, is expected to show the signature of advanced nucleosynthesis (Ventura et al. 2001).

Unfortunately, AGB modeling is highly uncertain, due to the strong sensitivity of the results obtained on the assumptions made concerning phenomena which are not known from first principles, the most relevant of which is convection (Ventura & D’Antona 2005a): the studies focused on the understanding of the thermal stratification within convective regions, and the extent of the third dredge up (TDU), i.e. the inwards penetration of the con-

---

Send offprint requests to: P. Ventura

vective envelope following each thermal pulse (TP), are far from reaching definitive and generalized conclusions. The description of mass loss also plays a fundamental role in the results obtained, whereas the chemical content of the ejecta for some light elements, in particular sodium, are extremely sensitive to the nuclear cross sections adopted (Ventura & D'Antona 2005b).

In this contribution we focus our attention on GCs of intermediate metallicity, and present the latest generation of AGB models calculated by means of the ATON code for stellar evolution, with the most updated physics inputs for what concerns the equation of state and the conductive opacities. The initial mixture is assumed to be  $\alpha$ -enhanced, to allow a better investigation of our working hypothesis.

The results obtained are compared with the observed abundance patterns of GCs stars. Our goal is to test if and under which assumptions it is possible to get ejecta from massive AGBs which may follow the patterns shown by the spectroscopic investigations of GCs: in particular, we will test the possibility of reproducing the O-Al and O-Na anticorrelations, which are the most analyzed in the literature. We disregard the Mg-Al anticorrelation, as it is still under debate (Cohen & Meléndez 2005), and we do not compare in details the fluorine yields with the observations, because  $^{19}\text{F}$  has been measured so far only in bright giants (Smith et al. 2005), so that a possible role played by some non canonical extra-mixing during the RGB phase in determining the small fluorine abundances observed cannot be ruled out.

## 2. The ATON code

The evolutionary sequences presented in this work have been calculated with the ATON code for stellar evolution. The interested reader may find in Ventura et al. (1998) a full description of the numerical structure of the code, with the recent updates given in Ventura & D'Antona (2005a).

The nuclear network includes 30 species, from hydrogen to silicon; all the reactions relevant for this study, involving the light elements

mostly investigated in the spectroscopic analysis of GC stars, are properly considered.

Mass loss can be modeled according to the traditional Reimers' recipe, or with the two prescriptions more appropriate to describe the stellar winds during the AGB phase, i.e. Vassiliadis & Wood (1993) and Blöcker (1995).

Convection is modeled locally, either with the traditional Mixing Length Theory (MLT) scheme (Vitense 1953), or by the Full Spectrum of Turbulence (FST) model (Canuto & Mazzitelli 1991). Within regions unstable to convection, nuclear burning is coupled with mixing by solving a diffusive-like equation (Cloutman & Eoll 1976): this approach, though more time consuming, is mandatory to allow a consistent description of the outer convective zone of AGBs, because a considerable fraction of the nuclear energy is generated within the envelope (Mazzitelli et al. 1999). The diffusive approach requires an alternative description of overshooting, which in this case is described as an exponential decay of convective velocities within the radiative regions, with an e-folding distance given by  $\zeta H_p$ , where  $\zeta$  is a free parameter.

The latest updates, specifically used for the present investigation, are the followings:

- The new OPAL (2005) equation of state<sup>1</sup> was implemented into the code
- The OPAL opacities (Iglesias & Rogers 1996) are overwritten in the low temperature regime ( $T < 10000\text{K}$ ) with the new opacities by Ferguson et al.(2005)
- We use the latest release of the conductive opacities by Potekhin (Cassisi et al. 2007)
- The mixture can be assumed to be solar scaled, or  $\alpha$ -enhanced, with  $[\alpha/\text{Fe}]^2 = +0.2, +0.4$

<sup>1</sup> Available at the WEB page <http://physci.llnl.gov/Research/>

<sup>2</sup> We use the standard notation: given the mass fraction  $X$  of a given element, and the iron abundance  $\text{Fe}$ , we define  $[\text{X}/\text{Fe}] = \log(\text{X}/\text{Fe}) - \log(\text{X}/\text{Fe})_{\odot}$ .

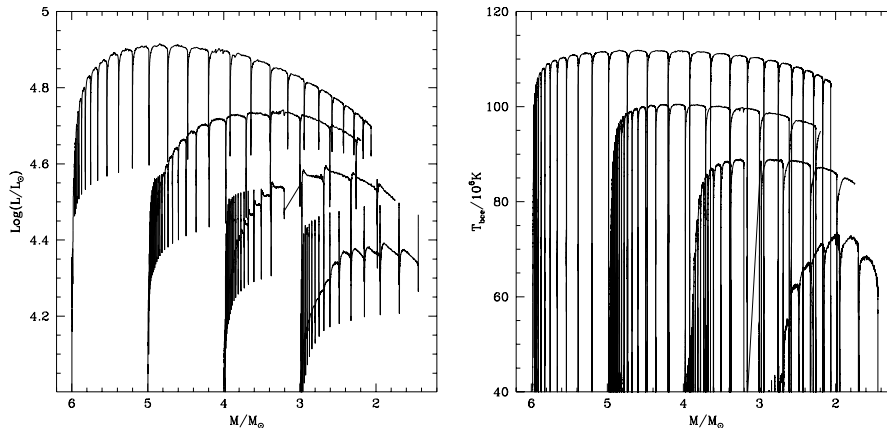


**Fig. 1.** Variation with the total mass of the luminosity (Left) and Temperature at the bottom of the convective envelope (Right) of some intermediate mass models during the AGB phase. For clarity reasons, only models corresponding to initial masses  $3, 4, 5, 6M_{\odot}$  are shown.

### 3. Results

We limit the present analysis to GCs of intermediate metallicity, with  $[\text{Fe}/\text{H}] \sim -1.3$ . We computed evolutionary sequences of initial mass  $3M_{\odot} \leq M \leq 6.3M_{\odot}$  with chemistry  $Z=0.001$  and  $Y=0.24$ . The lower and upper limits in mass are determined, respectively, by the absence of any HBB in masses with  $M < 3M_{\odot}$ , and by the off center carbon ignition in models more massive than  $6.3M_{\odot}$ . The evolutions are followed until the mass of the envelope becomes so small to prevent HBB, i.e.  $\sim 0.5 - 0.7M_{\odot}$ . Convection is modelled according to the FST treatment. The parameter giving the e-folding distance of the exponential decay of velocities inside radiative regions is  $\zeta = 0.02$ , in agreement with a calibration based on the observed widths of the main sequences of open clusters given in Ventura et al. (1998); no extra-mixing was assumed during the TDU. Mass loss was described via the Blöcker prescription, with the free parameter  $\eta_R$  entering the formula chosen as  $\eta_R = 0.02$ , according to a previous calibration based on the luminosity function of lithium rich stars in the Magellanic Clouds given in Ventura et al. (2000).

Fig.1 shows the evolution of the luminosity and the temperature  $T_{\text{bce}}$  at the bottom of the envelope of the models. We note the rapid

increase of the luminosity when  $T_{\text{bce}}$  exceeds  $\sim 40 \times 10^6 \text{K}$ , which is the temperature at which HBB occurs: this is typical of the AGB modeling based on the FST treatment of convection. We see in the right panel of Fig.1 that for each mass it is possible to fix a given  $T_{\text{bce}}$ , which remains approximately constant during the almost totality of the AGB evolution: this fixes the degree of the nucleosynthesis which is achieved at the bottom of the envelope. In the present study, the maximum temperature at the bottom of the envelope, found in the most massive models, is  $T_{\text{bce}} = 110 \text{MK}$ .

Table 1 gives the chemical content of the ejecta of the models discussed here. The high values of the helium mass fraction, particularly for the largest masses, are almost entirely due to the second dredge-up: this prediction is thus reliable, being independent of the choice of the free parameters entering the following AGB phase. The strong HBB achieved at the bottom of the envelope of these stars is also confirmed by the large depletion of fluorine, shown in col.5. Col.8 gives the ratio between the overall CNO content of the ejecta and the initial value: the most massive models, characterized by a strong mass loss and thus a small number of TPs, are expected to show only a

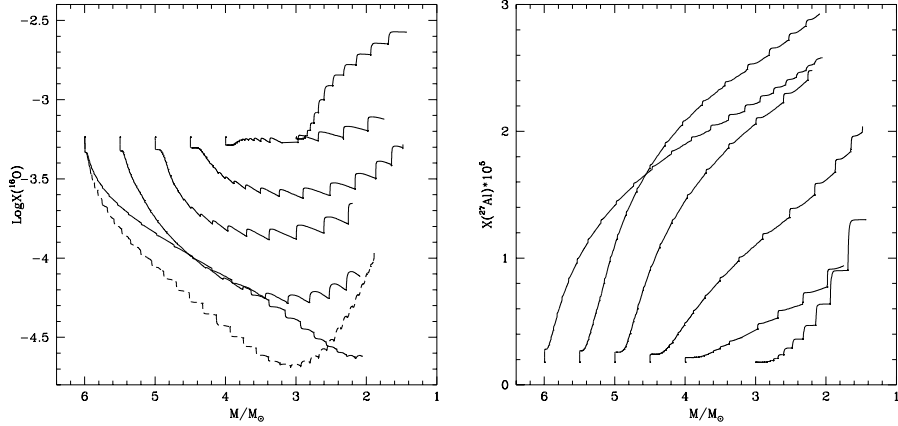


**Fig. 2.** Variation with the total mass of the surface abundances of oxygen (Left) and aluminium (Right) of some intermediate mass models during the AGB phase. For clarity reasons, models corresponding to initial masses  $3.5$  and  $6.3M_{\odot}$  were omitted. The dashed track corresponds to a  $6M_{\odot}$  model calculated with a lower mass loss ( $\eta_R = 0.01$ ).

modest increase of the CNO, due to the very few TDU episodes experienced.

The two panels of Fig.2 shows the variation of the surface abundances of oxygen (left) and aluminium (right) during the AGB phase; the choice of using the mass on the abscissa gives an idea of the chemistry of the ejecta. In the left panel we note that only masses  $M \geq 4.5M_{\odot}$  destroy oxygen at the surface, whereas the less massive models, due to the lower  $T_{\text{bce}}$  and the many TDUs, produce oxygen. Within the upper range of masses investigated here the oxygen yield is approximately independent of mass, because more massive models, being more luminous, suffer a stronger mass loss, thus loose more mass in the early AGB phase, when the surface oxygen abundance is still high (note the different slopes of the oxygen-mass trend corresponding to the  $5$  and  $6M_{\odot}$  cases in the left panel of Fig.2): this compensates the larger extent of the oxygen depletion determined by the larger  $T_{\text{bce}}$ . The dashed track, which represents a  $6M_{\odot}$  model calculated with a mass loss rate artificially decreased by a factor 2, shows that the oxygen yield is also independent of mass loss: when this latter is reduced, the tendency of the star to eject into the interstellar medium more oxy-

gen poor material, is compensated by the larger number of TPs experienced, which acts to increase the oxygen abundance.

The oxygen content of the ejecta of the most massive models is thus a very robust prediction of the present investigation, as it turns out to be practically independent of the uncertainties associated to mass loss, cross sections, and the exact upper limit of the initial mass of stars undergoing the AGB phase. Within the context of the self-enrichment scenario, we identify this oxygen abundance, which is found to be  $[\text{O}/\text{Fe}] = -0.4$ , with the oxygen content of the most oxygen poor stars observed in the GCs: if we limits this comparison to scarcely evolved stars, to rule out any possible additional contribution of some kind of extra-mixing acting during the RGB phase, we see a very good agreement between the theoretical predictions and the observational evidence, as can be seen by looking at the oxygen abundances of the stars shown in Fig.4.

Aluminium is produced in all AGBs (see the right panel of Fig.2), due to proton capture by the heavy magnesium isotopes, which are synthesized by HBB via  $^{24}\text{Mg}$  burning, and also dredged-up after each TP. Contrary to oxygen, the reliability of the results is undermined by

**Table 1.** Chemical composition of the ejecta of intermediate mass models

$M/M_{\odot}$	Y	A(Li)	[ $^{16}\text{O}/\text{Fe}$ ]	[ $^{19}\text{F}/\text{Fe}$ ]	[ $^{23}\text{Na}/\text{Fe}$ ]	[ $^{27}\text{Al}/\text{Fe}$ ]	R(CNO)
3.0	.248	2.77	0.92	0.10	1.16	0.65	9.6
3.5	.265	2.43	0.77	-0.26	1.30	0.66	7.9
4.0	.281	2.20	0.44	-0.61	1.18	0.55	4.9
4.5	.310	2.00	0.19	-0.90	0.97	0.85	3.1
5.0	.324	1.98	-0.06	-1.16	0.60	1.02	2.1
5.5	.334	1.93	-0.35	-1.39	0.37	1.10	1.3
6.0	.343	2.02	-0.40	-1.36	0.31	1.04	0.97
6.3	.348	2.06	-0.37	-1.28	0.30	0.99	0.94

the uncertainties associated to the relevant reactions rates (Izzard et al. 2007), which introduce an error on the theoretical predictions on  $[\text{Al}/\text{Fe}]$  of 0.3-0.4 dex; despite this, we confirm that massive AGBs produce great amounts of aluminium within their envelope (see col.7 of Table 1), the largest abundances, of the order of  $[\text{Al}/\text{Fe}] \sim 1$  dex, being for the most massive models of our sample. We note again that these results are in excellent agreement with the largest aluminium abundances detected in GCs stars, which in fact show up an increase by a factor 10 compared to the solar scaled abundance (Snedden et al. 2004).

We are left with sodium, which has been extensively measured in GCs stars. Fig.4 shows a clear oxygen-sodium anticorrelation, the stars most oxygen poor showing a sodium enrichment of the order of  $\sim 0.5$ dex. Unfortunately, the amount of sodium which may be produced within this class of objects is hard to predict, for the following reasons: a) the behavior of sodium is not linear, because it is first produced at the bottom of the envelope due to proton capture by  $^{22}\text{Ne}$  nuclei, and later destroyed when the destruction rate exceeds the production (see Fig.3); b) the uncertainties associated to the reaction rates are huge, of the order of 3 dex (Hale et al. 2002; 2004). Fig.3 compares the results in terms of the surface sodium abundance when the upper (solid) and lower (dotted) limits for the  $^{22}\text{Ne}(p,\gamma)^{23}\text{Na}$  are adopted: these results, completely different between each other, give an idea of the modest predictive power of our models on this issue.

Comparing our models with the observed abundances (see Fig.4), we may only conclude that when the larger cross-sections for proton

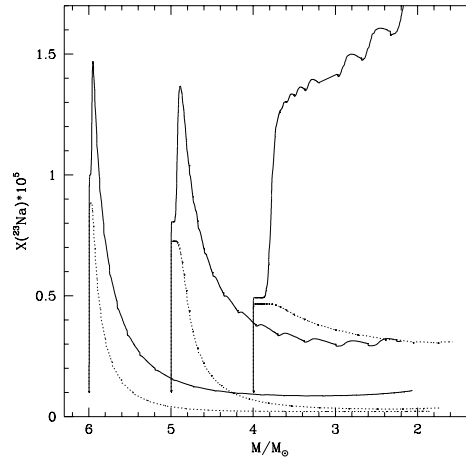


**Fig. 3.** The evolution with mass of the surface abundance of sodium for models of 4,5,6 $M_{\odot}$ . The dashed tracks indicate the results obtained when the lower limits of the cross sections of the reaction  $^{22}\text{Ne}(p,\gamma)^{23}\text{Na}$  are adopted.

capture by  $^{22}\text{Ne}$  nuclei are adopted, the yields of the most massive models are compatible with the observed abundances.

#### 4. Conclusions

We present the latest generation of AGB models of intermediate mass stars, and compare the chemistry of their ejecta with the observed surface abundances of GC stars.

The models are predicted to synthesize helium, with a maximum helium mass fraction produced in the envelopes of the most massive stars of the order of  $Y=0.35$ . The strong

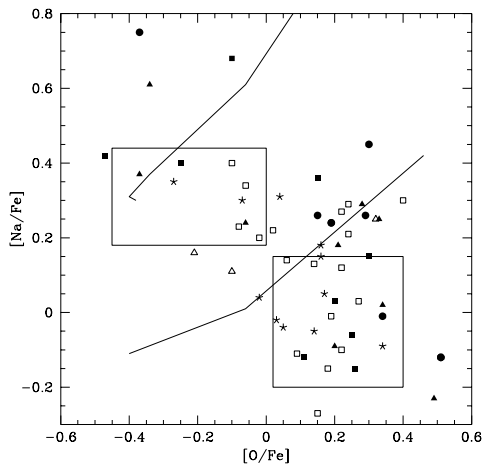


**Fig. 4.** The observed oxygen and sodium abundances observed in scarcely evolved GC stars of intermediate metallicity. The meaning of symbols is as follows: Full triangles: NGC 6752 (Gratton et al. 2001); Open squares: M5 stars with  $V > 16$  (Ramirez & Cohen 2003); Stars: M13 stars with  $V > 15$  (Cohen & Meléndez 2005); Open triangles: M3 stars with  $V > 15$  (Cohen & Meléndez 2005); Full points: NGC 6218 stars (Carretta et al. 2006); Open squares: High gravity M3 giants (Snedden et al. 2004); Full squares: High gravity M13 giants (Snedden et al. 2004). The upper and lower solid tracks indicate the theoretical predictions of our models when the upper and lower limits of the cross sections of the proton capture reactions by  $^{22}\text{Ne}$  nuclei are adopted.

HBB at the bottom of the outer convective zone determines an oxygen depletion in all models with masses  $M \geq 4.5M_{\odot}$ , with a minimum abundance  $[\text{O}/\text{Fe}] = -0.4$  occurring around  $M = 6M_{\odot}$ ; this prediction is robust, as it turns out to be practically independent of the description of mass loss.

The aluminium and sodium abundances are less reliable, due to the great uncertainties associated to the relevant proton capture cross sections. For aluminium, we find that proton capture by the heavy magnesium isotopes at the bottom of the envelope favors a great Al production, which reaches  $[\text{Al}/\text{Fe}] = +1$  for the

largest masses; this results may vary by  $\sim 30\%$  according to the choice of the relevant reaction rate.

The situation for sodium is far more uncertain, as the uncertainties on the cross sections at the temperatures of interest here reaches 3 order of magnitudes; the question whether these class of objects produces or destroy sodium is still open. However, with an appropriate choice of the cross sections, it is possible to produce ejecta which, for the masses in the range  $5\text{-}6M_{\odot}$ , are oxygen poor and sodium rich; since this matter is also expected to be aluminium rich and with a constant C+N+O content; we suggest that these stars are responsible for the pollution of the interstellar medium with gas from which the stars with the anomalous chemistry formed.

## References

- Blöcker, T. 1995, *A&A*, 297, 727  
 Canuto, V.M.C., & Mazzitelli, I. 1991, *ApJ*, 370, 295  
 Carretta, E. 2006, *AJ*, 131, 1766  
 Carretta, E., Bragaglia, A., Gratton, R.G., Leone, F., Recio-Blanco, A., & Lucatello, S. 2006 *A&A*, 450, 523  
 Cassisi, S., Potekhin, A.Y., Pietrinferni, A., Catelan, M., & Salaris, M. 2007, *ApJ*, 661, 1094  
 Cloutman, L., & Eoll, J.G. 1976, *ApJ*, 206, 548  
 Cohen, J.G., & Meléndez, J. 2005, *AJ*, 129, 303  
 Denissenkov, P., & Weiss, A. 2001, *ApJ*, 559, L115  
 Ferguson, J.W., Alexander, D.R., Allard, F., Barman, T., Bodnarik, J.G., Hauschildt, P.H., Heffner-Wong, A., & Tamanai, A. 2005, *ApJ*, 623, 585  
 Gratton, R., Bonifacio, P., Bragaglia, A., et al. 2001, *A&A*, 369, 87  
 Gratton, R., Sneden, C., & Carretta, E. 2004, *ARA&A*, 42, 385  
 Hale, S.E., Champagne, A.E., Iliadis, C., Hansper, V.Y., Powell, D.C., & Blackmon, J.C. 2002, *Phys.Rev.C*, 65, 5801  
 Hale, S.E., Champagne, A.E., Iliadis, C., Hansper, V.Y., Powell, D.C., & Blackmon, J.C. 2004, *Phys.Rev.C*, 70, 5802

- Iglesias, C.A., & Rogers, F.J. 2001, *ApJ*, 464, 943
- Ivans, I.I., Sneden, C., Kraft, R.P., et al. 1999, *AJ*, 118, 1273
- Izzard, R.G., Lugaro, M., Karakas, A.I., Iliadis, C., & van Raai, M. 2007, *A&A*, 466, 641
- Kraft, R.P. 1994, *PASP*, 106, 553
- Mazzitelli, I., D'Antona, F., & Ventura, P. 1999, *A&A*, 348, 846
- Ramirez, S.V., & Cohen, J.G. 2003, *AJ*, 125, 224
- Smith, V.V., Cunha, K., Ivans, I.I., Lattanzio, J.C., Campbell, S., & Hinkle, K.H. 2005, *ApJ*, 633, 392
- Sneden, C., Kraft, R.P., Guhathakurta, P., Peterson, R.C., & Fulbright, J.P. 2004, *AJ*, 127, 2162
- Vassiliadis, E., & Wood, P.R. 1993, *ApJ*, 413, 641
- Ventura, P., & D'Antona, F. 2005a, *A&A*, 431, 279
- Ventura, P., & D'Antona, F. 2005b, *A&A*, 439, 1075
- Ventura, P., D'Antona, F., Mazzitelli, I., & Gratton, R. 2001, *ApJ*, 550, L65
- Ventura, P., Zeppieri, A., D'Antona, F., & Mazzitelli, I. 1998, *A&A*, 334, 953
- Vitense, E. 1953, *Zs.Ap.*, 32, 135